ELSEVIER

Catalysis Today 61 (2000) 377–382

CATALYSIS TODAY

www.elsevier.com/locate/cattod

Oxidative dehydrogenation of isobutane over magnesium molybdate catalysts

Y.J. Zhang [a], I. Rodríguez-Ramos [a,*], A. Guerrero-Ruiz [b]

[a] *Instituto de Catálisis y Petroleoquímica, CSIC, Campus Cantoblanco, 28049 Madrid, Spain*
[b] *Departamento de Química Inorgánica, UNED, Paseo Senda del Rey 9, 28040 Madrid, Spain*

Abstract

A series of Mo-Mg-O catalysts with different crystalline phases (pure and mixtures) have been studied in the oxidative dehydrogenation of isobutane. X-ray diffraction, UV–Vis spectroscopy and temperature programmed reduction were applied to characterise the samples. In addition, the kinetics of the lattice oxygen exchange with labelled $C^{18}O_2$ was measured for all samples. It has been found that the $MgMoO_4$ phase contains the surface active sites suitable for the adsorption of isobutane and for its dehydrogenation to isobutene with the minimum of cracking reaction. Moreover, for this reaction the migration of lattice oxygen ions is not a key parameter in the control of the catalytic properties of these materials. © 2000 Elsevier Science B.V. All rights reserved.

Keywords: Oxidative dehydrogenation; Isobutane; Magnesium molybdate catalysts

1. Introduction

Metal molybdates are extensively used as catalysts for hydrocarbon partial oxidation and dehydrogenation reactions. In particular, magnesium molybdates have been studied in oxidative dehydrogenation of propane [1,2]. However, little is known in relation with the reaction mechanism or about the active sites present over this type of materials. In this sense, the performance of magnesium molybdate compounds in the oxidative dehydrogenation of propane have been related with MoO_x clusters formed on the surface of $MgMoO_4$ [3], and also the importance of the lattice oxygen ions in the control of selectivities has been indicated [2,4]. On the other hand, there is a current interest in the development and understanding of MoO_3/MgO catalysts [5,6], due to their high selectivity in the oxidation of butane to butadiene. This latter reaction is performed in the absence of oxygen [5], and studies by X-ray absorption techniques (EXAFS/XANES) have detected the presence of surface molybdate species $MgMoO_4$, which are transformed under high temperature calcination conditions from tetrahedral species, MoO_4, to octahedral one MoO_6 [6,7]. Notwithstanding, this type of mixed oxides has not been explored as catalysts for other selective oxidation reactions, for instance the isobutane dehydrogenation to isobutene.

In the recent years, we have attempted to relate the bulk oxygen mobility of catalytic oxides with the control of their selectivities in partial oxidation reactions. For instance, we have been able to identify differential oxygen migration rates in MoO_3 catalysts depending on their crystalline structure. In this way, the structure sensitive character of the partial oxidation of propylene to acrolein on MoO_3 samples can be ascribed to

---

[*] Corresponding author. Tel.: +34-1-5854765;
fax: +34-1-5854760.
E-mail address: irodriguez@icp.csic.es (I. Rodríguez-Ramos).

PII: S0920-5861(00)00398-9

a bulk property of this oxide, which varies with the crystalline structure [8]. The same line of reasoning has been applied to the V-Mg-O system. In this case the higher performance of the α-$Mg_2V_2O_7$ phase for the oxidative dehydrogenation of propane to propylene have been correlated with its decreased ability, in comparison with $Mg_3V_2O_8$ and β-MgV_2O_6 phases and pure V_2O_5, to furnish oxygen to the surface adsorbed species. By performing the oxygen isotopic exchange experiments among $C^{18}O_2$ gas molecules and the oxidic pure phases [9], it has been detected that the more selective phase exhibits decreased lattice oxygen mobility. Another important aspect of the partial oxidation reactions is the possibility of synergetic mechanisms, in which one phase helps the surface active sites placed on another phase by controlling the oxygen supply [10]. Thus, a special attention has to be paid to the preparation and characterisation of mixed oxides, as well as to the interpretation of the oxygen exchange reaction data.

In this study we have synthesised a series of mixed phases ($MgMo_xO_y$), either by solid reaction of MoO_3 with MgO or by coprecipitation–calcination. By the control of the relative amount of magnesium and molybdenum in the preparation, MgO or MoO_3 enriched samples (or supported on the more stable $MgMoO_x$ phase) have been obtained. The catalysts have been characterised by X-ray diffraction, temperature programmed reduction, surface area determination and UV diffuse reflectance spectroscopy. Furthermore, the oxygen ion mobility over some selected samples was determined by performing the oxygen isotopic exchange between the solids and $C^{18}O_2$. In this way, we have attempted to correlate the characterisation parameters, and particularly the oxygen exchange properties, with the catalytic properties.

2. Experimental

The synthesis of magnesium molybdates was carried out by solid reaction of reagent grade oxides MoO_3 and MgO (Fluka). Physical mixtures of these solids, with different MgO/MoO_3 molar ratios, were calcined at 897 K for 40 h. In one case, sample $0.15MgO/0.85MoO_3$, the final calcination temperature was increased up to 1073 K in order to favour the formation of $MgMo_2O_7$ phase [11]. Furthermore, some samples were prepared by coprecipitation [2] from aqueous solutions with pH=6 of $(NH_4)_6Mo_7O_{24}$ and $Mg(NO_3)_2$ (Aldrich), and further calcination at 897 K for 10 h. Table 1 describes the catalyst preparations and some characteristics of the resulting samples.

A part from the determination of specific surface area of the samples in an automatic instrument Micrometric ASAP 2000 (BET method applied to the isotherm of N_2 adsorption at 77 K); the catalysts were analysed by X-ray diffraction (XRD). The XRD patterns were recorded in a Siefert C-3000 diffractometer provided with a secondary monochromator and using Cu Kα radiation. The temperature programmed reduction (TPR) profiles of different samples under hydrogen flow were determined in a microbalance (CI Electronic) of 1 μg resolution. The UV–Vis diffuse reflectance spectra of the catalysts were measured in a Varian Cary I spectrophotometer equipped with a

Table 1
Preparation methods, compositions and some characteristics of the $MgMo_xO_y$ catalysts

Catalyst composition	Preparation method	Calcination conditions		S_{BET} ($m^2\ g^{-1}$)	Crystalline phase detected by XRD	Oxygen exchange slope values
		T (K)	t (h)			
MgO	–	–	–	51	MgO	–
MoO_3	–	–	–	0.2	MoO_3	0.00052
$0.3MgO/0.7MoO_3$	Solid reaction	897	40	0.4	$Mg_2O_3O_{11}$, MoO_3	–
$0.46MgO/0.54MoO_3$	Solid reaction	897	40	0.6	$Mg_2Mo_3O_{11}$, $MgMoO_4$	–
$0.15MgO/0.85MoO_3$	Solid reaction	1073	48	0.4	$MgMo_2O_7$, MoO_3	0.00096
$0.97MgO/1.0MoO_3$	Coprecipitation, pH=6	897	10	1.6	$MgMoO_4$	0.00084
$1.0MgO/1.0MoO_3$	Coprecipitation, pH=6	897	10	2.1	$MgMoO_4$	0.00049
$1.03MgO/1.0MoO_3$	Coprecipitation, pH=6	897	10	2.2	$MgMoO_4$	–
$2.0MgO/3.0MoO_3$	Coprecipitation, pH=6	897	10	0.9	$Mg_2Mo_3O_{11}$, $MgMoO_4$	0.00178

diffuse reflectance attachment and operated in the range 200–900 nm.

Oxygen exchange experiments with $C^{18}O_2$ (Isotec, isotopic purity 95%) were carried out using 50–100 mg of the sample held inside a quartz reactor coupled to a grease-free standard vacuum system [9]. The gas phase was analysed by an on-line mass quadrupole spectrometer (Balzers QMG 421C) connected to the reactor through a metering leak valve. In these experiments the gas phase is recirculated through the sample bed by a low volume stainless steel mechanic pump. The exchange reaction was performed at 723 K using percentages of ^{18}O atoms in the system ($\%^{18}O = 2N(C^{18}O_2)_{gas}/[2N(C^{18}O_2)_{gas} + xN(M^{16}O_x)]$, where N is the number of gas molecules, and x the number of oxygen atoms for each metal oxide) close to 12%. Under these conditions after an initial surface oxygen exchange reaction, which will depend on the surface area of solids, the slopes of the isotopic labelling of gaseous CO_2 curves F (^{18}O) versus time can be directly related to the bulk oxygen ion migration rates [9]. F (^{18}O) is defined as: $[I(46)+2I(48)]/2[I(44)+I(46)+I(48)]$, where I is the intensity of the mass quadrupole peak corresponding to the m/z values given in parenthesis.

The catalytic properties of the samples in the oxidative dehydrogenation of isobutane were evaluated using a fix-bed reactor, consisted in an U-shaped quartz tube (inner diameter 0.5 cm and length 20 cm). About 0.2 g of the catalyst was placed between two quartz–wool plugs and pretreated under an oxygen/helium mixture at 773 K. Reactant feed gas contained 2.7% O_2, 8.2% isobutane and balance He with a total flow of 46 cm^3/min. The effluent gases from the reactor were analysed by an on-line gas chromatograph (Varian 3400) equipped with TCD and FID detectors, and a 20% BMEA on Chromosorb P-AW column for the separation of components. The catalytic properties were studied under isobutane conversions lower than 10% at two reaction temperatures, 803 and 823 K. The carbon balance of the main products was 98±2% and blank tests showed no conversion of isobutane when no catalyst was present in the reactor.

3. Results and discussion

Table 1 shows the preparation conditions, composition and surface area of the different magnesium molybdate samples. The XRD patterns of the samples are displayed in Fig. 1 and the crystalline phases detected are summarised in Table 1. In general the obtained surface area of the solids are rather low

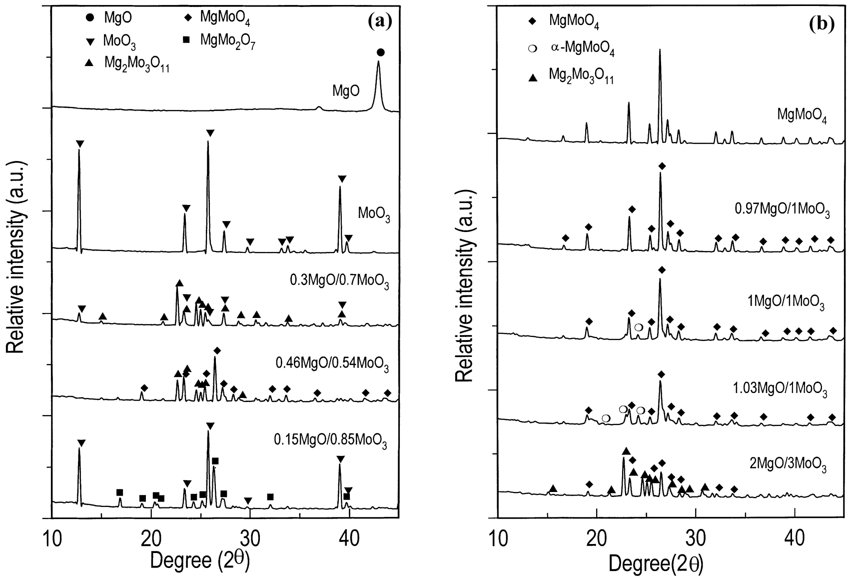

Fig. 1. XRD patterns of MgO, MoO_3 and the different magnesium molybdate samples.

(below 3 $m^2\,g^{-1}$). Various magnesium molybdates can be found among the crystalline phases. Samples prepared from aqueous solutions and with compositions close to the stoichiometric show a pure crystalline phase ($MgMoO_4$) but all others show mixtures of two crystalline phases. With this latter series of samples, we will be able to detect cooperative effects, if any. It should be noted, however, that amorphous phases and/or surface enrichments are not determined by XRD. For instance, in a sample prepared with excess of MgO ($1.03MgO/1.0MoO_3$) the presence of MgO is not detected by XRD and the same occurs for the excess of MoO_3 in the $0.97MgO/1.0MoO_3$ sample.

The nature of molybdenum species after calcination was determined from the diffuse reflectance spectra in the UV region. It is known that the energy charge transfer bands for the molybdenum ions, which are related to charge transfer between molybdenum and oxygen, are strongly affected by the coordination and oxidation states of molybdenum [12,13]. Thus, while two absorption bands of Mo^{6+} ions with tetrahedral coordination are observed at 230 and 270 nm, the larger band in the 310–370 nm region is associated with the octahedral coordination of the Mo ions. An unambiguous assignment of UV–Vis features is very complicated but from Fig. 2, we can indicate that the magnesium molybdate samples do not display the characteristic band of bulk MoO_3 centred at 340 nm. Moreover, we find for samples with excess of MoO_3 ($0.3MgO/0.7MoO_3$ and $0.15MgO/0.85MoO_3$) two broad bands at 250 and above 290 nm, this latter band is probably related to small MoO_3 clusters [3]. Finally, for all samples with stoichiometric amounts of MgO and MoO_3 in the composition ($0.97MgO/1.0MoO_3$, $1.0MgO/1.0MoO_3$, $1.03MgO/1.0MoO_3$) the recorded spectra are similar to that reported in Fig. 2 for $0.46MgO/0.54MoO_3$ sample. They only show a large peak centred at 250 nm corresponding to Mo^{6+} in tetrahedral coordination. From the TPR profiles, not presented here for the sake of brevity, we can indicate that the reduction of magnesium molybdate phases starts at temperatures between 720 and 790 K, which are significantly lower than the corresponding MoO_3. Thus, we can deduce that the reducibility under hydrogen of tetrahedral Mo^{6+} ions is higher than that of octahedral Mo^{6+} species. However, based on the TPR, we were unable to detect differences in surface reactivity induced by the surface enrichment with MgO or MoO_3.

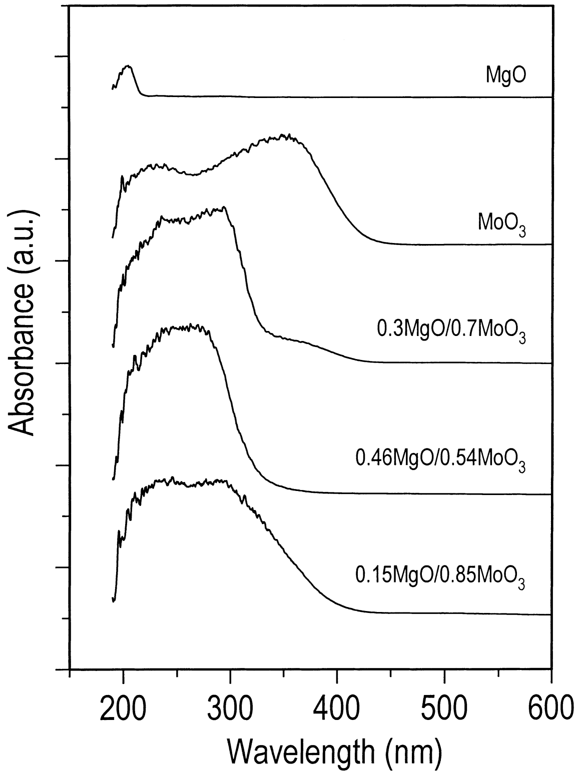

Fig. 2. UV diffuse reflectance spectra of MgO, MoO_3 and some magnesium molybdate samples.

As a representative data of the catalytic behaviour, in Table 2 are shown the catalytic conversions and the selectivities achieved on the different magnesium molybdate samples. Two values of selectivity are given for the different products obtained at the reaction temperatures of 803 and 823 K. In the case of isobutene selectivity the lower value corresponds to 823 K reaction temperature and the higher to 803 K, and the opposite is found for the rest of the products. It is seen that the isobutene selectivity at 803 K for MgO is the lowest one (39%), although it is higher over MoO_3 (65%) a significant increase over this parameter is obtained with the $1.0MgO/1.0MoO_3$ solid containing only the $MgMoO_4$ phase (84%). The presence of MgO over the $MgMoO_4$ phase, $1.03MgO/1.0MoO_3$ catalyst, reduces the selectivity of isobutene to 70%. The $0.97MgO/1.0MoO_3$ catalyst has a slight excess

Table 2
Oxidative dehydrogenation of isobutane over various magnesium molybdate catalysts

Catalyst	Isobutane conversion (%)		Selectivity (%)			
	At 803 K	At 823 K	Isobutene	Propene	Methane	CO_x
MgO	6	8	39–37	25–32	0–3	28–36
MoO_3	2	4	65–60	23–30	6–8	6–2
$0.3MgO/0.7MoO_3$	1	3	69–64	22–26	5–7	4–3
$0.46MgO/0.54MoO_3$	3	4	77–70	15–21	4–5	4–4
$0.15MgO/0.85MoO_3$	1	4	68–64	22–27	6–7	4–2
$0.97MgO/1.0MoO_3$	7	8	80–72	10–16	3–4	7–8
$1.0MgO/1.0MoO_3$	6	8	84–76	4–9	1–2	11–13
$1.03MgO/1.0MoO_3$	2	4	66–62	19–25	4–6	11–7
$2.0MgO/3.0MoO_3$	6	9	81–73	7–11	2–3	10–13

of MoO_x not detected by XRD and the isobutane selectivity is slightly reduced to 80%. The diminution in selectivity with excess of MgO is higher than with excess of MoO_3, because the former is much less selective. In our approach, we have synthesised samples with different MgO/MoO_3 ratios and have detected the effect of the MgO or MoO_3 presence at the $MgMoO_4$ surface over the catalytic properties. The $0.46MgO/0.54MoO_3$ and $2.0MgO/3.0MoO_3$ samples, which contains the $MgMoO_4$ phase, also have a high selectivity to isobutene, close to 80%. From these results and in opposition to the effects detected for the oxidative dehydrogenation of propane over $MgMo_xO_y$ catalysts [3], we suggest that the $MgMoO_4$ phase (without the presence of surface MoO_x clusters) contains the surface active sites suitable for the adsorption of isobutane and for its dehydrogenation to isobutene with the minimum of secondary reactions. From Table 2, we can also indicate that for this reaction and this type of catalysts it appears that cooperative or synergetic effects between phases ($Mg_2Mo_3O_{11}+MgMoO_4$, $Mg_2O_3O_{11}+MoO_3$, $MgMoO_4+MoO_3$) do not seem to take place. Another important aspect is the high production of the secondary product, propylene. Besides isobutene, the high surface area MgO produces propylene and carbon oxides, while the low surface area MoO_3 mainly yields methane along with propylene. Probably in both cases the high reactivity of the primary product, isobutene, causes the formation of the secondary prod-

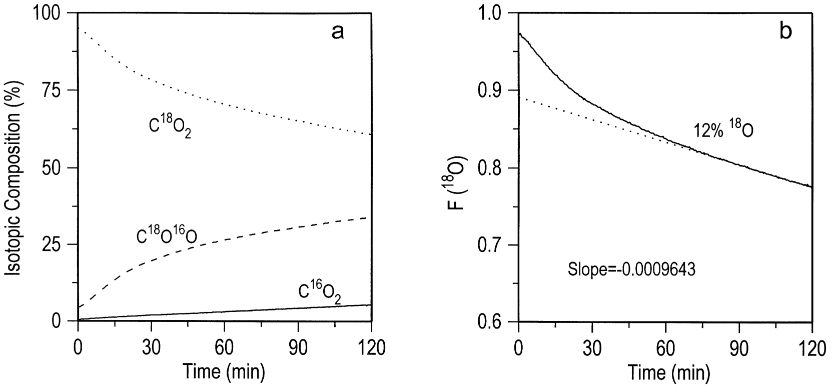

Fig. 3. Oxygen exchange reaction between $C^{18}O_2$ and $0.15MgO/0.85MoO_3$ sample: (a) isotopic composition versus time in the reaction; (b) isotopic labelling of gaseous CO_2 during the reaction (full line) and fitted slope (dotted line).

ucts. The lower isobutene selectivity of the MoO_3 (and catalysts wherein this phase is detected) compared with the $MgMoO_4$ phase can be related with its higher activity for the isobutene cracking to give propylene.

On the other hand, we have also attempted to correlate the catalytic selectivity of these samples with the oxygen mobility in the bulk of these mixed oxides. The results obtained for the sample $0.15MgO/0.85MoO_3$ in its isotopic oxygen exchange with $C^{18}O_2$ at 723 K are represented in Fig. 3. Considering that the slope of the F (^{18}O) versus time plot is informative of the oxygen diffusion [8,9,14,15], the obtained slope values for various samples are given in Table 1. These slope values cannot be related either with the catalytic activities or with the selectivities. Thus, for this reaction the migration of lattice oxygen ions is not a key parameter in the control of the catalytic properties of these materials.

In conclusion, the isobutane oxidative dehydrogenation over magnesium molybdate catalysts seems to require only surface sites consistent in tetrahedral Mo^{6+} sites (or reduced species from them). In the case of samples containing MoO_3, and in general octahedral Mo^{6+}, probably partially reduced (Mo^{5+}) or coordinatively unsaturated surface sites are responsible for their catalytic properties. Moreover, it is found that compared to MoO_3 the $MgMoO_4$ phase has a decreased ability for the cracking of isobutene to yield propylene and methane. Under the experimental conditions of this work, the oxygen mobility through the bulk oxides and the synergetic phenomena (in samples with more than one phase) play a minor role in the control of the catalytic selectivity.

Acknowledgements

This work was supported by a joint project of the CAS (Chinese Academy of Sciences) and the CSIC (Consejo Superior de Investigaciones Científicas). Y.-J. Zhang thanks the AECI (Agencia Española de Cooperación Internacional) for a postdoctoral fellowship.

References

[1] M.C. Abello, M.F. Gomez, L.E. Cardus, Catal. Lett. 43 (1997) 229.
[2] Y.S. Yoon, W. Ueda, Y. Moro-oka, Catal. Lett. 35 (1995) 57.
[3] K.H. Lee, Y.S. Yoon, W. Ueda, Y. Moro-oka, Catal. Lett. 46 (1997) 267.
[4] Y.S. Yoon, N. Fujikawa, W. Ueda, Y. Moro-oka, K.W. Lee, Catal. Today 24 (1995) 327.
[5] G.E. Vrieland, C.B. Murchison, Appl. Catal. A 134 (1996) 101.
[6] S.R. Bare, Langmuir 14 (1998) 1500.
[7] H. Shimada, N. Matsubayashi, T. Sato, Y. Yoshimura, A. Nishijima, N. Kosugi, H. Kuroda, J. Catal. 138 (1992) 746.
[8] A. Guerrero-Ruiz, I. Rodríguez-Ramos, P. Ferreira-Aparicio, M. Abon, J.C. Volta, Catal. Today 32 (1996) 223.
[9] A. Guerrero-Ruiz, I. Rodríguez-Ramos, P. Ferreira-Aparicio, J.C. Volta, Catal. Lett. 45 (1997) 113.
[10] B. Delmon, Stud. Surf. Sci. Catal. 112 (1997) 1.
[11] V.G. Zubkov, I.A. Leonidov, K.R. Poeppelmeier, V.L. Kozhevnikov, J. Solid State Chem. 111 (1994) 197.
[12] L. Wang, W.K. Hall, J. Catal. 77 (1982) 232.
[13] K. Marcinkowska, L. Rodrigo, S. Kaliaguine, P.C. Roberge, J. Mol. Catal. 33 (1985) 189.
[14] H. Kakioka, V. Ducarme, S.J. Teichner, J. Chem. Phys. 68 (1971) 1715.
[15] Y. Iizuka, M. Sanada, J. Tsunetoshi, N. Yamaguchi, S. Arai, J. Chem. Soc., Faraday Trans. 90 (1994) 1307.